Testing bulk models of icosahedral quasicrystals with STM images of clean surfaces

Zorka Papadopolos, Oliver Groening, Roland Widmer

Testing bulk models of icosahedral quasicrystals with STM images of clean surfaces

Journal:	*Philosophical Magazine & Philosophical Magazine Letters*
Manuscript ID:	TPHM-07-Dec-0357.R2
Journal Selection:	Philosophical Magazine
Date Submitted by the Author:	06-Jun-2008
Complete List of Authors:	Papadopolos, Zorka; Eberhard-Karls Universität, Institut für Theoretische Physik Groening, Oliver; EMPA, Abt. 127 Widmer, Roland; EMPA Thun, nanotech@surfaces
Keywords:	quasicrystalline alloys, quasicrystals
Keywords (user supplied):	quasicrystalline alloys, quasicrystals
Note: The following files were submitted by the author for peer review, but cannot be converted to PDF. You must view these files (e.g. movies) online.	
ZPapadopolos-TelAviv2007-paper-revised2.tex	

Philosophical Magazine,
Vol. 00, No. 00, DD Month 200x, 1–8

Testing bulk models of icosahedral quasicrystals with STM images of clean surfaces

Zorka Papadopolos*, Roland Widmer#, Oliver Gröning#

*Institut für Theoretische Physik, Universität Tübingen, Germany,

#EMPA, Swiss Federal Laboratories for Materials Testing and Research, Nanotech@Surfaces Laboratory, Thun, Switzerland

(June 6, 2008)

In the case of the icosahedral Al-Pd-Mn we compare the STM (scanning tunnelling microscopy) image of the real fivefold surface to the STM simulations on the candidates of the fivefold bulk terminations. We make the choice, which termination fits the best to the real image. Among other conclusions we get some hints important either for the chemistry of the bulk-model or for the eventual correction of the model of atomic positions itself. We work in the frame of the particular model of atomic positions, based on the diffraction data for $Al_{70}Pd_{21}Mn_9$ and $Al_{62}Cu_{25.5}Fe_{12.5}$. We also discuss the possibilities beyond this model.

1 Introduction

Since 1999 we have studied the clean surfaces of quasicrystals (in particular icosahedral Al-Pd-Mn) comparing their STM images to the bulk terminations (see Ref. [1] and the references quoted therein), assuming that the shining spots on the STM (scanning tunnelling microscopy) images are the atoms/groups of atoms (e.g. the shining pentagons of an edge length of circa 3 Å).

In 2005 the first simulations [2] of the STM images were performed on the model $\mathcal{M}(\mathcal{T}^{*(2F)})$ [3], see Ref [4]. The model of atomic positions $\mathcal{M}(\mathcal{T}^{*(2F)})$, that we shortly define in Section 2, describes simultaneously icosahedral Al-Pd-Mn and Al-Cu-Fe. In Ref. [1], and in this paper, through the comparison of the STM images of the clean surfaces to the simulations of the STM on different candidates for the bulk terminations, we discuss also the validity of the model $\mathcal{M}(\mathcal{T}^{*(2F)})$ itself.

The LEED (low energy electron diffraction) images of the clean surfaces on different quasicrystals show the sharp Bragg peaks, ordered in a pattern supported by an expecting module, with the symmetry for the surface in question. These facts prove that the clean surfaces of quasicrystals are themselves also quasicrystalline. On the highly resolved STM images (in the direct space, $\mathbb{E}_{\|}$) the shining points are also placed on appropriate module points and the interatomic distances are as expected from the models, what encourage us to assume that a clean surface of the quasicrystal in question is not reconstructed, i.e. it is as in the bulk, hence, shell be well represented by some of the predicted bulk terminations, if the underlying bulk model is correct.

In Section 3 we define the bulk terminations via a generalisation of Bravais' rule. In case of quasicrystals, the several ångström thick atomic layers of highest densities, instead of the planes, are the terminations. This concept we broadly discussed in Ref. [5].

On the surfaces one observes the small, local configurations of the highest symmetry, the "clusters" and their long range order. We interpret the most of the 2-dimensional "clusters" on the surface as an intersection of the 3-dimensional "clusters" in the bulk model by the surface (top) plane of the termination. This conclusion does not speak in favour of the "cluster-nature" of quasicrystals.

It turned out [5] that there are two alternative Fibonacci sequences of possible fivefold bulk terminations in the model $\mathcal{M}(\mathcal{T}^{*(2F)})$. In Ref. [1] we searched in both sequences for an appropriate termination, such that the simulation of the STM is as close as possible to the STM image. The termination that fits at best by the appearance of the 2-dimensional "clusters', turned out not to be rich in Al atoms in the surface (top) plane, what is against the model independent LEIS (low energy ion scattering) results [6, 7]. It brought us to the conclusion, under the assumption

*Corresponding author. Email: zorka.papadopolos@uni-tuebingen.de

Philosophical Magazine
ISSN 1478-6435 print/ISSN 1478-6443 online © 200x Taylor & Francis
http://www.tandf.co.uk/journals
DOI: 10.1080/1478643YYxxxxxxxx

that the model of the atomic positions $\mathcal{M}(\mathcal{T}^{*(2F)})$ is correct, the Al atoms in the present model are wrongly placed. In Section 3 we present in short this reasoning from Ref. [1]. Additionally we show the appearance of the STM simulations on several different possible terminations from the chosen, correct sequence of the terminations. We learn from these images that the definition of one of the frequent local configurations, that we call the "dark star" and label by dS, must be generalised.

In particular, in Section 5 we discuss also a possibility that the model of the atomic positions needs not to be fully deterministic. With somewhat changed model of the possible atomic positions, one might be able to keep roughly the present placement of the Al atoms.

2 A model of the atomic positions of icosahedral Al-Pd-Mn and Al-Cu-Fe

We assume the variant of the Katz-Gratias-Boudard model, $\mathcal{M}(\mathcal{T}^{*(2F)})$, see Ref. [1, 3, 8] and Refs quoted therein. The model is based on the diffraction results of the Boudard model [9] and of the Katz-Gratias model [10]. The same model of atomic positions describes $Al_{70}Pd_{21}Mn_9$ and $Al_{62}Cu_{25.5}Fe_{12.5}$ [11].

The model $\mathcal{M}(\mathcal{T}^{*(2F)})$ of icosahedral quasicrystals of an F-phase is obtained through the decoration of the icosahedral tiling $\mathcal{T}^{*(2F)}$ by the icosahedral atomic configurations, clusters, in shape of the Bergman and the Mackay polyhedra [1, 3, 8].

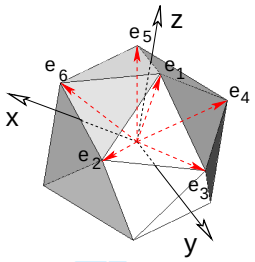

Figure 1. With $e_i, i = 1, 2 \ldots 6$ is usually denoted the standard $\mathbb{Z}_6$ basis $\{e_i \mid (e_i, e_j) = \delta_{i,j}, i, j = 1, \ldots 6\}$. Here, by $e_i, i = 1, 2 \ldots 6$ we mean the icosahedrally projected basis vectors to $\mathbb{E}_{\|}$, $\{(e_i)_{\|}\}$, as is clear from the geometry of the image. The projected basis vectors are along the fivefold symmetry axes of the icosahedron, drown in red colour. We use this "fivefold coordinate system" whereas the authors in Refs [9–12] use the "threefold coordinate system", equivalent to the basis $\{e_1, e_2, e_3, e_4, -e_5, e_6\}$. x-, y- and z-axes are the twofold symmetry axes of the icosahedron.

Table 1. Points $x = \frac{1}{2}(N_1, \ldots, N_6)$ of D_6^{ω} lattice ($N_i, i = 1, \ldots, 6$ are integers), reciprocal to D_6, split into four classes with respect to the D_6 translations. The symbol E denotes an even integer and O an odd one.

class-criterion*	Ref. [3]	Ref. [10]	Refs [9, 11, 12]
$\frac{1}{2}(E_1, \ldots, E_6)$; $\frac{1}{2}\sum_i E_i = E$	q	n'	n_0
$\frac{1}{2}(E_1, \ldots, E_6)$; $\frac{1}{2}\sum_i E_i = O$	b	n	n_1
$\frac{1}{2}(O_1, \ldots, O_6)$; $\frac{1}{2}\sum_i O_i = O$	a	bc	bc_1
$\frac{1}{2}(O_1, \ldots, O_6)$; $\frac{1}{2}\sum_i O_i = E$	c		

* It is the class-criterion w. r. t. the fivefold coordinate system, as in Fig 1.

The deterministic [1] model of atomic positions is defined by the *module*, the three copies of the icosahedrally projected D_6 lattice, and the corresponding *windows* (atomic surfaces), see Fig. 2, that defines the three quasilattices of atomic positions, labelled by b, a and q, see also Table 1. The model is a union of these three quasi lattices. The volumes of the windows are in a proportion $Vol(W_b) : Vol(W_a) : Vol(W_q) = (6\tau + 8) : 1 : (8\tau + 2)$, $\tau = (1 + \sqrt{5})/2$, which define the relative frequencies of the b, a and q sites in the model $\mathcal{M}(\mathcal{T}^{*(2F)})$.

To specify the scale in the model, we use the standard distances, denoted by ⑤, ② and ③ along the fivefold, twofold and threefold axes respectively, which are related by ③ $/\sqrt{3} =$ ⑤ $/\sqrt{\tau + 2} =$ ② $/2$ $(= 1/\sqrt{2(\tau + 2)})$, in which $\tau = (1 + \sqrt{5})/2$. The standard distances are used in both the observable space $\mathbb{E}_{\|}$ and the coding space

[1] A model is deterministic if all the possible atomic positions are occupied by the atoms.

$\mathbb{E}_\perp$. The lines and intervals along the fivefold directions, if marked in colour, are in red, along twofold blue, and along threefold yellow. The standard distance ⑤ $(= 1/\sqrt{2})$ in $\mathbb{E}_\parallel$ is set to be 4.561 Å for i-AlPdMn and 4.465 Å for i-AlCuFe.

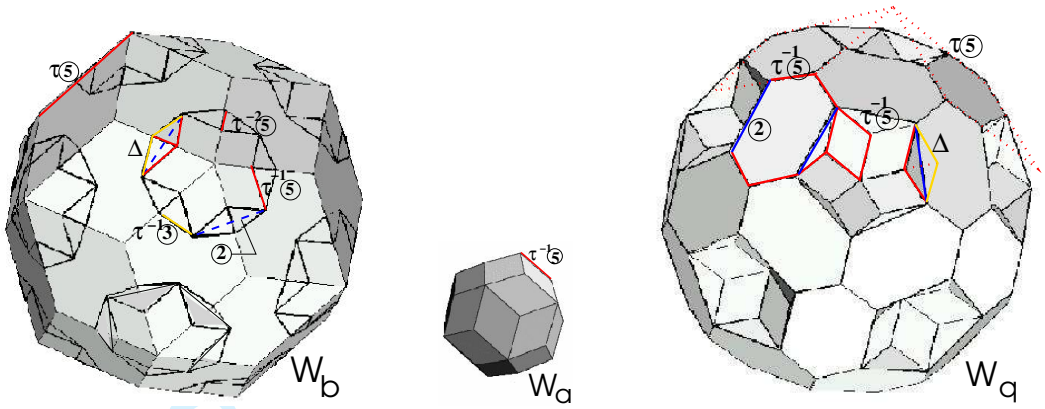

Figure 2. The final windows W_b, W_a, W_q in the coding space $\mathbb{E}_\perp$ define the deterministic geometric model $\mathcal{M}(\mathcal{T}^{*(2F)})$ of atomic positions based on the icosahedral D_6 module M_F. (*left*) W_b is obtained on taking the marked tetrahedra (Δ) away from the triacontahedron of edge length τ⑤. The tetrahedron Δ has a mirror symmetry plane and edges: two of length τ^{-1}⑤, one of length τ^{-2}⑤, two of length τ^{-1}③ and one of length ②. The mirror plane is orthogonal to the twofold edge and contains the single edge of length τ^{-2}⑤. (*middle*) W_a is a triacontahedron of edge length τ^{-1}⑤. (*right*) W_q with edge lengths τ^{-1}⑤ and ② $= 2$⑤$/\sqrt{\tau+2}$, $\tau = (1+\sqrt{5})/2$. The windows fulfil the closeness condition: i. e., there are no forbidden (short) distances in the model.

The windows in Fig. 2 fulfil the closeness condition: the interatomic distances in $\mathbb{E}_\parallel$ along the main symmetry directions, fivefold, threefold and twofold are not shorter than τ^{-1}⑤, τ^{-1}③ and τ^{-1}②, respectively [13].

The windows of Katz-Gratias model [10] could be easily obtained from our windows if the tetrahedra Δ would not be taken away from the window W_b, but instead, from the window W_q.

3 Fivefold surfaces and corresponding bulk terminations

The most stable clean surfaces of icosahedral Al-Pd-Mn (i-AlPdMn) and of icosahedral Al-Cu-Fe (i-AlCuFe) are the fivefold surfaces [14]. These are *terrace-stepped* [15]. The fivefold surfaces (orthogonal to the fivefold symmetry axis) present sequences of flat terraces with characteristic terrace step heights of circa $m = 4.08$ Å and $l = 6.60$ Å, see Fig. 3.

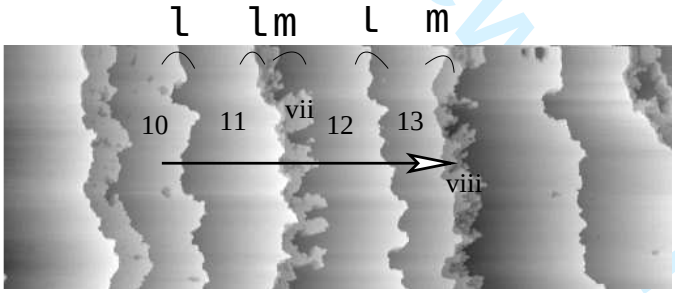

Figure 3. An STM image of a fivefold surface, size $1750 \times 648\,\mathrm{nm}^2$, of i-AlPdMn done by J. Ledieu. A Fibonacci-like sequence of the step heights of circa $m = 4.08$ Å and $l = 6.60$ Å was measured on this surface [16]. The marked subsequence of steps l, l, m, l, m from left - right, downwards, corresponds to a subsequence of the (q, b, b, q)-terminations in $\mathcal{M}(\mathcal{T}^{*(2F)})$ from Fig. 5 (*right*). Numbers 10, 11, 12 and 13 label the terminations coded by the window W and the numbers vii and viii label the terminations coded by the complement of W in τW, see Fig. 4 (*right*), Fig. 5 (*right*) and Table 3.

An important feature of the planes orthogonal to the main symmetry directions in any model based on two or more copies of the icosahedral D_6 module is, the atomic positions $x = \frac{1}{2}(N_1, \ldots, N_6)$ ($N_i, i = 1, \ldots, 6$ are integers) in a single fivefold or threefold plane belong to a single class, but twofold planes might contain atomic positions of all classes, as explained in Table 1 in Ref [17]. In the present paper we consider only the fivefold terminations. Hence, we introduce the property only for the fivefold planes in Table 2. It is clear that the projections of all points

from a single fivefold plane onto the unit vector $n_{\|}^5$, normal to the plane, are equal. This constant can be written $n_{\|}^5 \cdot x_{\|} = (N + M\tau)[\kappa_5]$, where N and M are two integer constants and $\kappa_5 = ⑤/\sqrt{5}$. The expression $N + M\tau$ for the points (atomic positions) in different classes can only take values as in Table 2. Hence, in a single plane only the points of the single class can coexist, the plane is coded by a *single* window, see Fig. 2.

Table 2. Independent of the shape of the atomic surfaces, the atomic positions, $x = \frac{1}{2}(N_1, \ldots, N_6)$, in a single fivefold plane of a model, based on the three copies of the icosahedral D_6 modules, belong to a single class, q, b or a. A unit vector normal to a fivefold plane is denoted with $n_{\|}^5$. The symbol E denotes an even integer and O an odd one. The scalar products are given in the unit $\kappa_5 = ⑤/\sqrt{5}$, where ⑤ is the standard distance along the fivefold axis. For the coordinate system see Fig. 1.

Class label	b	a	q
$n_{\|}^5 \cdot x_{\|}\ [\kappa_5]$	$O + E\tau$	$E + O\tau$	$E + E\tau$

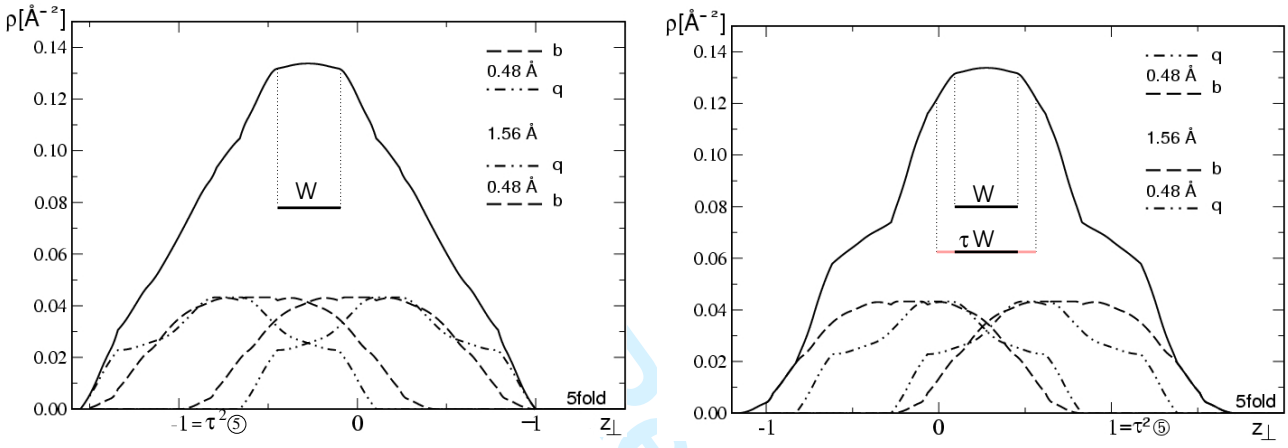

Figure 4. (*left*) Density graph $\rho_{5f}(z_\perp)$ of the fivefold (b, q, q, b)-layers, with spacings as in the image. The symbol ⑤ is the standard distance along a fivefold axis. (*right*) Density graph $\rho_{5f}(z_\perp)$ of the fivefold (q, b, b, q)-layers, with spacings as in the image. The supports of the plateaus in cases (*left*) and (*right*) are equally broad W, and encode the Fibonacci sequence with step heights $l = 6.60$ Å and $L = m + l = 10.68$ Å. The plateaus are equally high, i.e. the terminations are equally dense, but the density graph (*left*) is slightly steeper in the region $\tau W/W$, $\tau = (1 + \sqrt{5})/2$, than in case (*right*), where we mark the region $\tau W/W$ in pink (gray).

According to Bravais' rule, which is generally valid for crystals, the most stable surfaces are the densest atomic planes in the bulk. In [5] we observed among the fivefold planes in the model $\mathcal{M}(\mathcal{T}^{*(2F)})$ that the 2.52 Å thick atomic layers of (equal) maximum density appear in correct sequences, as the terrace-like sequences of the fivefold surfaces. This *thick* layer that contains four fivefold planes with spacings q_1-plane, 0.48 Å, b_1-plane, 1.56 Å, b_2-plane, 0.48 Å, q_2-plane is a candidate for a fivefold termination. The labels q and b mark the atomic positions belonging to different translational classes with respect to the D_6 lattice in the 6-dimensional space, see Tables 1 and 2. For the bundle we define an effective (averaged) *planar* density of internally contained thin layers[1]/planes

$$\rho_{5f}(z_\perp) = (1/2)[(\rho_{q_1}(z_\perp) + \rho_{b_1}(z_\perp)) + (\rho_{q_2}(z_\perp) + \rho_{b_2}(z_\perp))]. \quad (1)$$

In the coding space $\mathbb{E}_\perp$, $\rho_{5f}(z_\perp)$ is the smooth density graph, see Fig. 4. The density graph has a plateau. The support of the plateau, which is W broad, marks the layers with equal maximum densities, the candidates for the **terminations**. Each module point in the support along the fivefold symmetry axes $z_\perp$ in the coding $\mathbb{E}_\perp$ space (Fig. 4) corresponds one to one to $z_{\|}$, a position of the penetration of a fivefold symmetry axis (in observable $\mathbb{E}_{\|}$ space) into a single terminating layer (the position of a top-plane of a termination), as in Fig. 5. The height of the

[1] Under a *thin layer* we consider a layer of 2-3 planes of stacked atoms, on a distance significantly smaller than 0.86 Å. Such a layer we treat as a single plane.

Table 3. A list of some of the (q,b,b,q)-terminations and the single candidate of a (b,q,q,b)-termination. The symbol T-No (termination number) is the label of the candidates of the terminations, as in Fig. 5. The symbol $z_{\parallel}$ is the position of the top-plane of a termination along the fivefold z-axis, as it is listed in the patch of the model [3]. The symbol $z_{\perp}$ is the z-axis in $\mathbb{E}_{\perp}$, as in Fig. 4. The symbol $\rho(t-Pl)$ denotes the density of the top-plane in the termination, $\rho(-0.48$ Å$)$ the density of the plane 0.48 Å below the surface.

T-No	3_{qbbq}	2_{bqqb}	ii_{qbbq}	4_{qbbq}	6_{qbbq}	10_{qbbq}	11_{qbbq}	vii_{qbbq}	12_{qbbq}	13_{qbbq}	$viii_{qbbq}$
$z_{\parallel}$ [Å]	50.0	48.0	45.9	39.3	22.0	-16.6	-23.2	-29.8	-33.9	-40.5	-44.6
$z_{\perp}$ $[\tau^2$⑤$]$	0.19	0.36	0.53	0.32	0.24	0.42	0.21	0.00	0.34	0.13	0.47
$\rho(t-Pl)$ [Å^{-2}]	0.08	0.08	0.05	0.06	0.07	0.05	0.07	0.09	0.06	0.08	0.05
$\rho(-0.48$ Å$)$ [Å^{-2}]	0.06	0.06	0.09	0.08	0.07	0.08	0.06	0.03	0.08	0.05	0.08

plateau in Fig. 4 defines the density of the terminations to be 0.134 Å^{-2}. Note that it is an average planar density in the 2.52 Å thick (q,b,b,q)-layer below the surface, as in Equation 1.

But, one can bundle the dense (b,q) and (q,b) plane-like fivefold layers, buckled planes, into a 2.52 Å bundle (b,q,q,b) as well. For the layer we define an effective density as in the case of the (q,b,b,q)-layer.

The height and the width of the plateau on the density graph for the fivefold bundle (q,b,b,q) are of the same size as for the bundle (b,q,q,b), see Fig. 4. The width is $W=\frac{2\tau}{\tau+2}$ ⑤ and encodes the Fibonacci sequence of terrace heights $l=\frac{2\tau^2}{\tau+2}$⑤$=6.60$ Å and $L=\tau l=10.68$ Å. But the density graph of the layer (b,q,q,b) is slightly steeper in the region which is the complement of W in τW $(\tau W/W)$ than the graph of the layer (q,b,b,q) and causes that the appearance of the terrace height 4.08 Å is less probable to appear. For that reason we declared in Ref. [5] that the support of the plateau of the density graph in the case of the (q,b,b,q) atomic layers defines the sequence of the fivefold bulk terminations. On the terrace like fivefold surface all steps of a Fibonacci-like sequence from Fig. 3 have been measured [16]. The step heights are circa $m=4.08$ Å and $l=6.60$ Å. We identify an exact Fibonacci subsequence of steps l,l,m,l,m from left - right, downwards (see Fig. 3) that corresponds to a subsequence of the (q,b,b,q)-terminations in $\mathcal{M}(\mathcal{T}^{*(2F)})$ from Fig. 5 (*right*). The numbers 10, 11, vii, 12, 13 and viii label the fivefold terminations in the model that correspond to the terraces on the surface. In the subsequence, the terraces of the small area (labelled by vii and viii), the less stable terraces, correspond to the less dense terminations, according to the graph in Fig. 4 (*right*) are coded in the region which is the complement of W in τW $(\tau W/W)$, marked in pink (gray). These terminations are related to the $m=4.08$ Å steps. See also Fig. 5 (*right*) and Table 3.

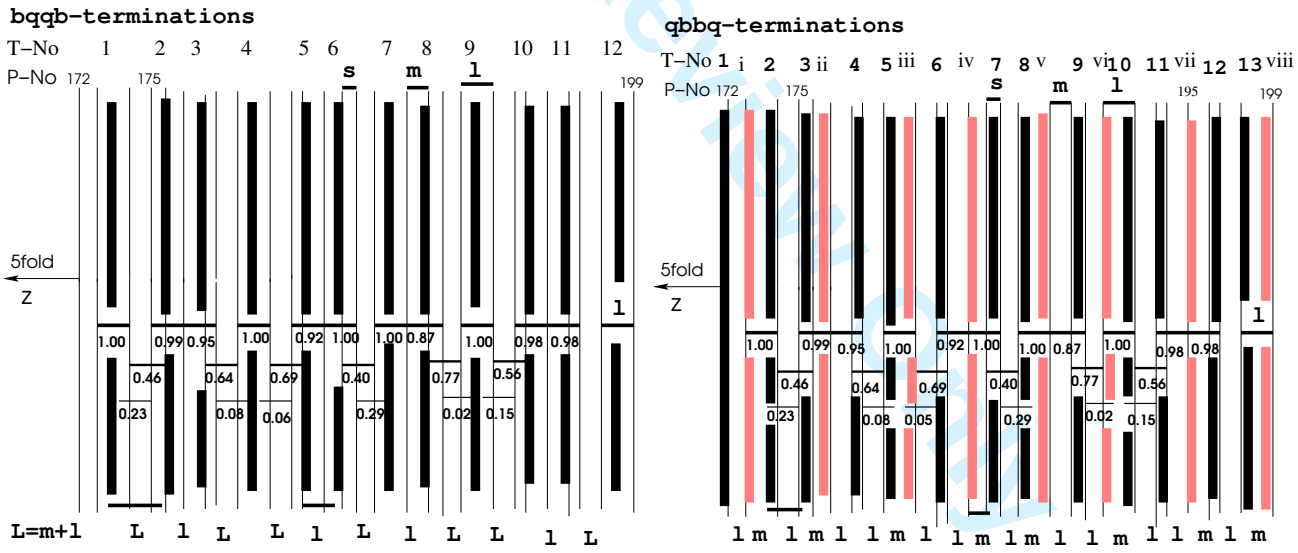

Figure 5. In the finite segment of $\mathcal{M}(\mathcal{T}^{*(2F)})$ thin lines mark the fivefold tiling $\mathcal{T}^{*(2F)}$ planes, labelled from 172 to 199. The distances between the tiling planes in case of i-AlPdMn are $s=2.52$ Å, $m=\tau s$ and $l=\tau m$, $\tau=(1+\sqrt{5})/2$. The fivefold layers of 6.60 Å broad Bergmans are marked by the l-intervals. Below each is written its relative density. (*left*) The Fibonacci sequence $\{l,\ L=l+m\}$ of the (b,q,q,b)-termination candidates presented relative to the sequence of the fivefold planes of the tiling. The terminations are numerate by the termination numbers (T-No). (*right*) The Fibonacci sequence $\{m,l\}$ of the (q,b,b,q)-termination candidates presented relative to the sequence of the fivefold planes of the tiling. We numerate these by the Arabic T-No. In gray (pink) are possible less dense termination candidates and should appear as smaller terraces on a surface, these are coded by the the region $\tau W/W$ marked also in pink (gray) in Fig. 4 (*right*).

In Fig. 5 we show the positions of the fivefold atomic layers 2.52 Å thick as candidates for the fivefold bulk

terminations, relative to the positions of the layers of the 6.60 Å broad Bergman polyhedra in the model. The fivefold layers of Bergmans, 6.60 Å$= l$ broad, are marked in the figure with the l-intervals.

According to Fig. 5, the most stable fivefold terminations (independent of which candidate, (q, b, b, q) or (b, q, q, b) is the correct fivefold termination) in the model pass *through* the dense layers of the Bergman polyhedra; hence these can not be energetically stable clusters. Similar argument is valid for the Mackay polyhedra. Analogous results are applicable for any icosahedral quasicrystal described with the $\mathcal{M}(\mathcal{T}^{*(2F)})$ model, in particular for i-AlCuFe [10].

4 Clusters on fivefold bulk terminations

The model independent LEIS (low energy ion scattering) investigations confirm that the surface of i-AlPdMn is rich in Al. At near grazing incidence LEIS shows the top plane surface composition to be about 95% Al [6] The amount of Pd increases and Al decreases as one probes deeper, giving an overall range of 88-96% Al obtained from LEIS results [6,7]. For that reason, in the STM simulations on both candidates for the terminations, on the (b, q, q, b)- and on the (q, b, b, q)-layers of maximum density we consider the same topographic contrast for all atomic positions regardless of their chemical nature. We set all atoms to be Al atoms. Further on, up to the scale, these images present STM simulations of *any* compound described with the model of atomic positions $\mathcal{M}(\mathcal{T}^{*(2F)})$. The STM simulations are based on a simplified atomic charge model [2], in which a spherical shape of the valence charge density is assumed for the atoms. This low level STM simulation serves the purpose of comparing geometrical features on a large area of a surface. The present ab initio calculations can not manage such a large set of data. And under the assumption that the recently published Ref. [18] is correctly reformulating the quantum chemistry, the "simplified atomic charge model" from Ref. [2] might become a real atomic charge model.

By the STM simulations of a fivefold surface [1, 4] we compared the proposed candidates for the terminations from the sequence of the layers (b, q, q, b) of maximum density to the sequence of the (q, b, b, q)-layers of an equal maximum density. The simulations of the two chosen layers, compared to the highly resolved STM image of a clean surface of i-AlPdMn we presented in [1, 4]. Here we repeat this reasoning and present in Fig. 6 several interesting simulated surfaces.

On the STM image (Fig. 6 (*11*)) one notices two characteristic fivefold symmetric configurations, the "white flower" (wF) and the "dark star" (dS) defined as in Refs [19] and [20]. The "white flower", the "dark star" and also the "ring" (R) configuration are seen on the simulations as well. The long range pattern of the dS and wF on the STM image, Fig. 6 (*11*) is evidently best reproduce by the simulations on the layers 3_{qbbq} (Fig. 6 (*12*) and Table 3) and 2_{bqqb} (Fig. 6 (*13*) and Table 3). But, the "white flowers", and in particular the "dark stars" are better reproduced on the (q, b, b, q)-layers as in Fig. 6 (*12*), (*22*) and (*23*). For example, a candidate of the dS on these (q, b, b, q)-layers is a Bergman cluster intersected by the surface plane, on (b, q, q, b)-layer it is a Mackay cluster intersected by the surface plane, and looks rather like a dark pentagon, and not like a star. Hence, we have discovered [1, 4] a confirmation that the maximum dense fivefold (q, b, b, q)-layers are the fivefold bulk terminations in the model $\mathcal{M}(\mathcal{T}^{*(2F)})$.

In Fig. 6 (*21*) we present the simulation on a lower density termination ii_{qbbq}, drown in pink (gray) in Fig. 5 (*right*). Moreover the top-plane in the termination is of a lower density than the plane 0.48 Å below (see Table 3). On this termination can exist neither the wF nor the R configuration, defined as in [20]. One concludes it from Fig. 5 (*right*), there is no layer of Bergman polyhedra direct under the surface, starting by the top plane in the termination. According to our old definition of the configuration dS, as in [19], that dS presents an intersection of the Bergman cluster by the top plane in the termination, such that the further five clusters in the bulk directly under the surface surround this intersection symmetrically by the five shining pentagonal faces of the Bergman clusters, on the ii_{qbbq}-termination none of the dS configurations should appear. But that is evidently wrong, because we observe many dS-like configurations on this termination on the positions where the Bergman clusters are cut by the top plane of the termination. Hence, we are forced to generalise the definition of dS: it should appear wherever a Bergman cluster is intersected by the top plane in the termination, i. e.,

$$dS \equiv cB. \tag{2}$$

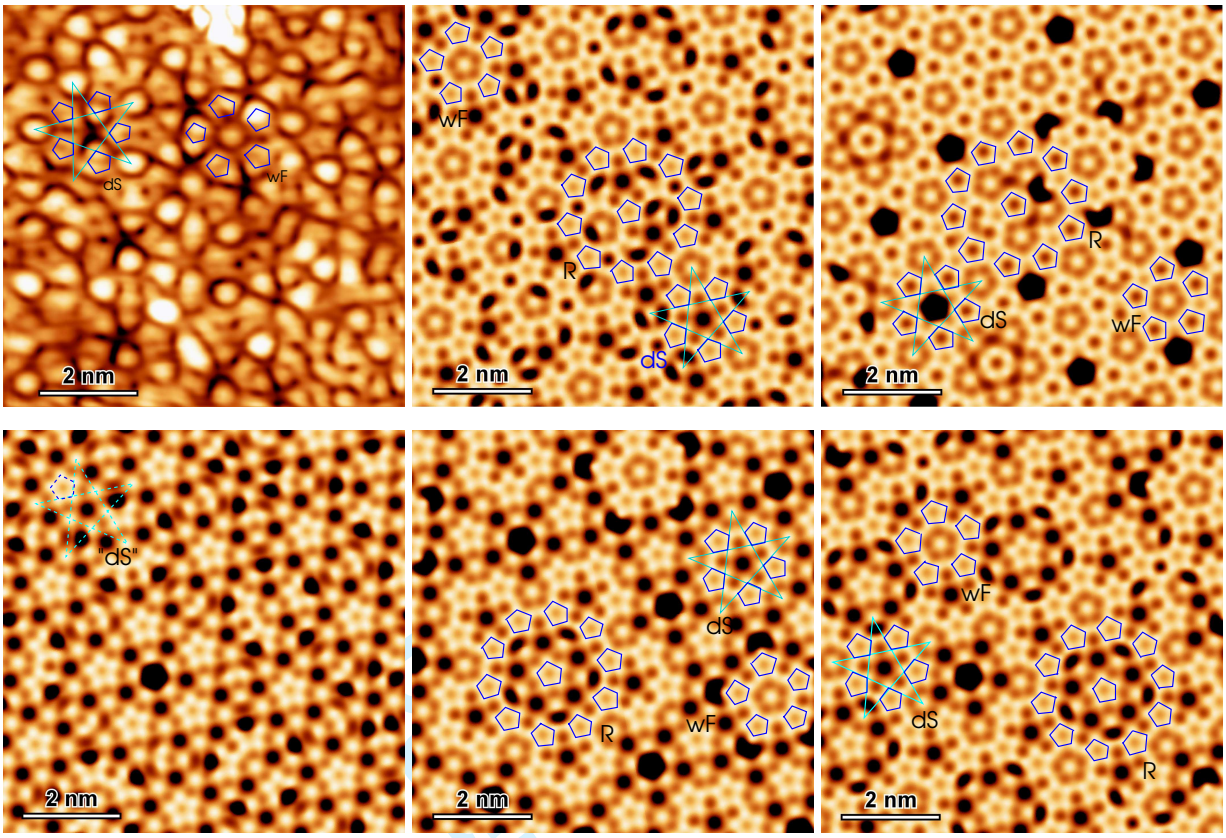

Figure 6. We label the six images in the figure like a 2×3 matrix: (*11*) An STM image of the fivefold clean surface of i-AlPdMn, with the marked representative fivefold symmetric local configurations "dark star" (dS) and the "white flower" (wF). The other images present the STM simulations performed on different candidates for the terminations. Using the labelling of the terminations, T-No as in Fig. 5 (*right*) and Table 3: (*12*) is on 3_{qbbq}, (*13*) on 2_{bqqb}. Note that this termination we rotated by 180° w. r. t. the others!, (*21*) on ii_{qbbq}, (*22*) on 4_{qbbq}, (*23*) on 6_{qbbq}. Each of the images is 80×80 Å^2. The candidates of the observed *fivefold symmetric* local configurations, "white flower" (wF) and the "dark star" (dS), and also the "ring" (R) are marked on the simulations. The edge of the pentagons marked in dark blue is $\tau^{-1}② = 2.96$ Å. Whereas dS appears on a chosen (b, q, q, b)-termination No 2_{bqqb} as a dark pentagon, it looks indeed like a dark pentagonal star on all the (q, b, b, q)-terminations. The same local configurations were observed on the STM images of the fivefold surface of i-AlCuFe as well.

For the definition of "cB" see Figs 10 and 11 in Ref. [19]. With this knowledge one determines easily the density of the dark stars on a termination

$$\rho(dS) = \rho(cB), \tag{3}$$

where cB labels a Bergman polyhedron cut by the surface-plane. The relative densities of the cB for a particular termination one reads easily from the Fig. 5, as for example

$$\rho_{2_{qbbq}}(dS) : \rho_{3_{qbbq}}(dS) : \rho_{6_{qbbq}}(dS) = 1 : 0.46 : 0.69. \tag{4}$$

The maximum density 1 corresponds to the absolute density of 0.013 Å^{-2}.

Notice that in Ref. [21] on the low-order periodic approximants to the icosahedral Al-Pd-Mn authors performed also the Tersoff-Hamann STM simulation [2]. Their result, presented in Fig. 2 of Ref. [21] places the fivefold surface on the dense layers rich in Al atoms in the top plane of the termination. And it is, in all current models, on the (b, q, q, b)-layers of maximum density. Their result corresponds to our image on Fig. 6(*13*).

5 The wrong chemistry or the wrong windows?

As we stated, from the LEIS investigations [6, 7] we know that the top q-plane in the terminating layer must be rich in Al atoms, but it is not the case in the model [3, 9–11]. Hence, the conclusion that the terminations are

the (q,b,b,q)-layers of maximum density contradicts the chemistry of the model $\mathcal{M}(\mathcal{T}^{*(2F)})$, adopted from the Boudard model. In case of i-AlCuFe, it contradicts the chemistry adopted from Katz-Gratias model.

In the above conclusion, we supposed that the model of the atomic positions (without chemistry) is correct. The reason of the different appearance of the pentagonal local configurations dS and wF in the simulations on the (q,b,b,q)-layer compared to the (b,q,q,b)-layer is because of the different **outer shape** of the windows W_b and W_q, see Fig. 2. More accurately, one compares the intersections of the windows W_b and W_q by the fivefold planes in $\mathbb{E}_\perp$. These intersections are the polygons that are coding the quasilattices in the fivefold b- and the q-planes in the 0.48 Å broad layer (a buckled plane) on the surface of the terminations. Whereas the coding of a dense b plane is by a disc like polygon, the q plane is coded by the pentagonal star-like polygon. See for example Fig. 12 in Ref. [19].

If, from the results on the diffraction the Al atoms in the model *must* be predominantly placed on the atomic surface W_b, as it is now [3,9–11], the shapes of the atomic surfaces (windows) must be changed. Roughly speaking, the shapes of W_q and W_b windows (from Fig. 2) should be exchanged. Hence, if the chemistry of the Boudard model [9] (which is a model with approximate windows) is kept, the deterministic models of the atomic positions, as by Katz and Gratias [10] and the model $\mathcal{M}(\mathcal{T}^{*(2F)})$ must be changed. Such a model has already been suggested by Fang et al. [12]. See in particular Figs 3 and 4 in Ref. [12]. But the new model [12] introduces the forbidden (too short) interatomic distances. In order to exclude these, some of the atomic positions in $\mathbb{E}_\parallel$ have to be considered as probabilistic. In $\mathbb{E}_\perp$ that means that not all the areas of the windows (atomic surfaces) in Figs 3 and 4 of Ref. [12] dare to be 100% filled.

6 Acknowledgements

Z. Papadopolos thanks G. Kasner for the graphs presented in Fig. 4, J. Ledieu for the STM image presented in Fig. 3, and acknowledges the financial support of Prof. H. Reinhardt (Univ. Tübingen). O. Gröning and R. Widmer thank M. Feuerbacher for providing the icosahedral Al-Pd-Mn monograin used in the STM work presented in Fig. 6 and acknowledge financial support from the Swiss National Science Foundation (SNF) under contract 200021-112333/1.

References

[1] Z. Papadopolos, O. Gröning and R. Widmer, "Clusters in F-phase icosahedral quasicrystals", in: *Models, Mysteries and Magic of Molecules*, Eds Jan C. A. Boeyens and John F. Ogilvie, Springer 2008, p. 255.
[2] J. Tersoff and D. R. Hamann, *Phys. Rev. B* **31**, (1985) 805.
[3] http://www.quasi.iastate.edu/Structure%20Dbase%20Info.html
[4] O. Gröning, R. Widmer, P. Ruffieux and P. Gröning, *Philos. Mag.* **86**, (2006) 773.
[5] Z. Papadopolos and G. Kasner, *Phys. Rev. B* **72**, (2005) 094206.
[6] C. Jenks, J. Whaley, R. Bastasz, unpublished results.
[7] C. J. Jenks, A. R. Ross, T. A. Lograsso, J. A. Whaley, and R. Bastasz, Surf. Sci. **521**, (2002) 34; C. J. Jenks and R. Bastasz Prog. Surf. Sci. **75**, (2004) 147.
[8] Z. Papadopolos, P. Kramer and W. Liebermeister, in *Proc. of the Int. Conf. on Aperiodic Crystals, Aperiodic 1997*, edited by M. de Boissieu, J.-L. Verger-Gaugry and R. Currant (World Scientific, Singapore, 1998), p. 173.
[9] M. de Boissieu, P. Stephens, M. Boudard, C. Janot, D. L. Chapman and M. Audier, *J. Phys.: Condens. Matter* **6**, (1994) 10725.
[10] A. Katz and D. Gratias, in *Proc. of the 5th Int. Conf. on Quasicrystals*, eds. C. Janot and R. Mosseri (World Scientific, Singapore, 1995) p. 164.
[11] V. Elser, *Philos. Mag. B* **73**, (1996) 641.
[12] A. Fang, H. Zou, F. Yu, R. Wang and X. Duan, *J. Phys.: Condens. Matter* **15**, (2003) 4947.
[13] Z. Papadopolos, G. Kasner, P. Kramer and D. E. Bürgler in: Mat.Res.Soc.Symp.Proc. Vol. 553, "Quasicrystals", Boston 30.11.-02.12.1998, eds: Jean-Marie Dubois, Patricia A. Thiel, An-Pang Tsai and Knut Urban, p. 231.
[14] Z. Shen, W. Raberg, M. Heinzig, C. J. Jenks, V. Fournée, M. A. Van Hove, T. A. Lograsso, D. Delaney, T. Cai, P. C. Canfield, I. R. Fisher, A. I. Goldman, M. J. Kramer and P. A. Thiel, *Surf. Sci.* **450**, (2000) 1.
[15] T.M. Schaub, D.E. Bürgler, H.-J. Güntherodt, J.B. Suck, *Phys. Rev. Lett.* **73**, (1994) 1255.
[16] J. Ledieu, E. J. Cox, R. McGrath, N. V. Richardson, Q. Chen, V. Fournée, T. A. Lograsso, A. R. Ross, K. J. Caspersen, B. Unal, J. W. Evans, P. A. Thiel, *Surf. Sci.* **583**, (2005) 4.
[17] Z. Papadopolos, P. Pleasants, G. Kasner, V. Fournée, C. J. Jenks, J. Ledieu and R. McGrath, Phys. Rev. B **69**, (2004) 224201.
[18] Jan C.A. Boeyens, *Z. Naturforsch.* **62b**, (2007) 373.
[19] Z. Papadopolos, G. Kasner, J. Ledieu, E. J. Cox, N. V. Richardson, Q. Chen, R. D. Diehl, T. A. Lograsso, A. R. Ross and R. McGrath, *Phys. Rev. B* **66**, (2002) 184207.
[20] G. Kasner, Z. Papadopolos, *Philos. Mag.* **86**, (2006) 813.
[21] M. Krajči, J. Hafner, J. Ledieu, and R. McGrath, *Phys. Rev. B* **73**, (2006) 24202.

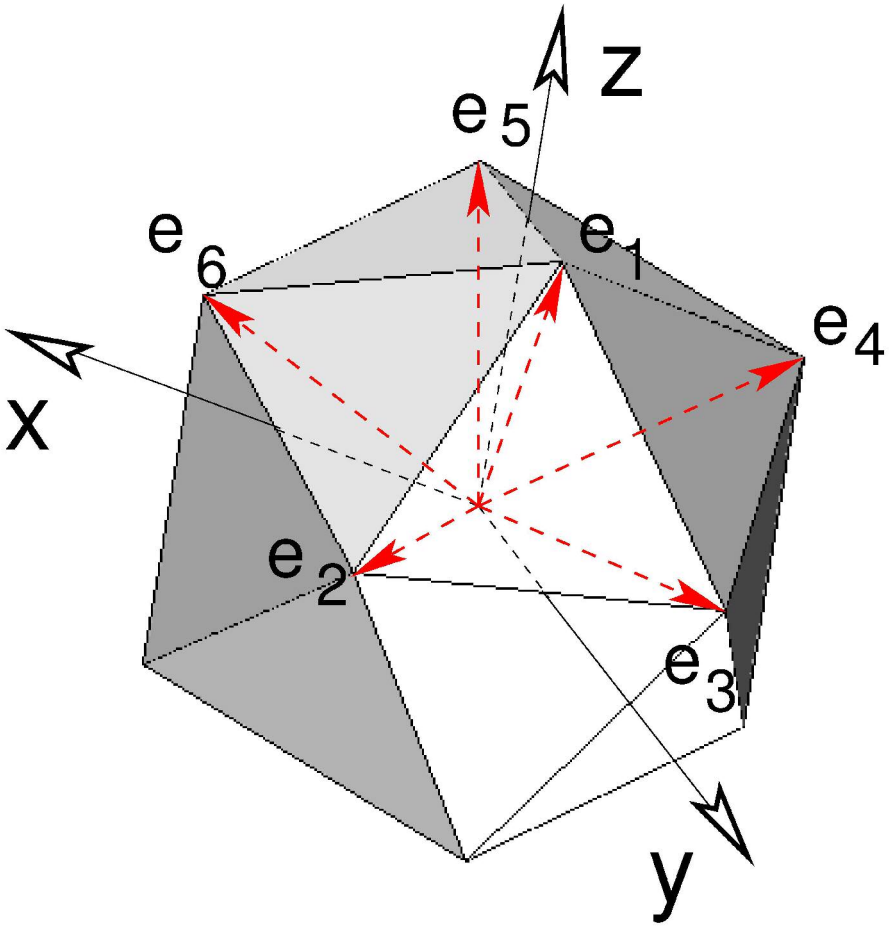

141x142mm (600 x 600 DPI)

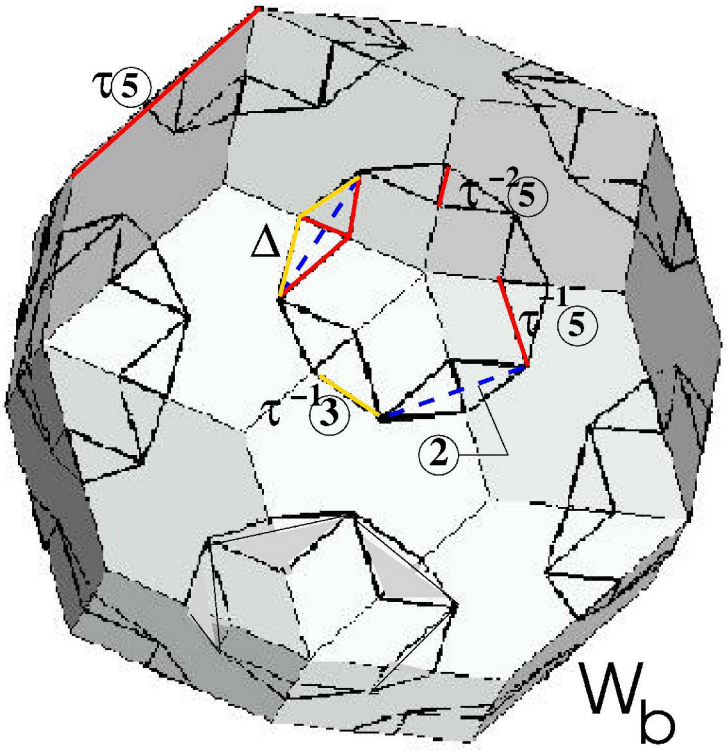

160x144mm (600 x 600 DPI)

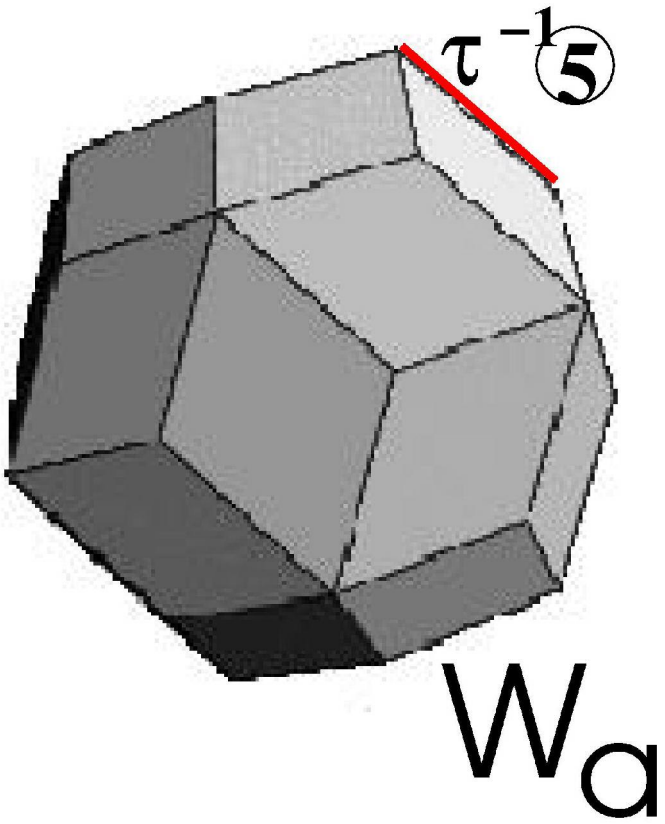

82x82mm (600 x 600 DPI)

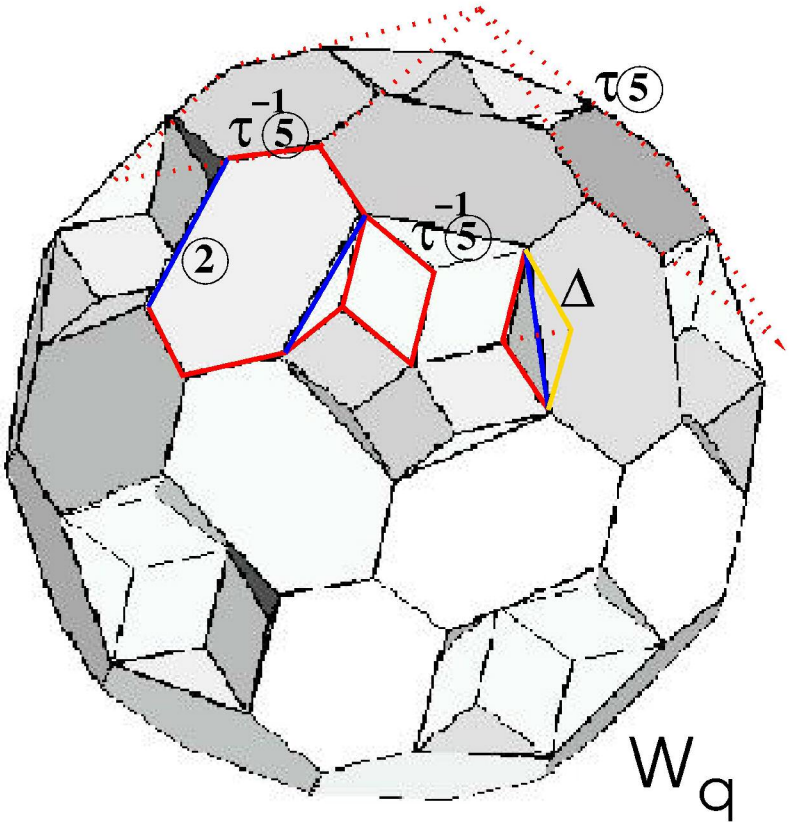

138x137mm (600 x 600 DPI)

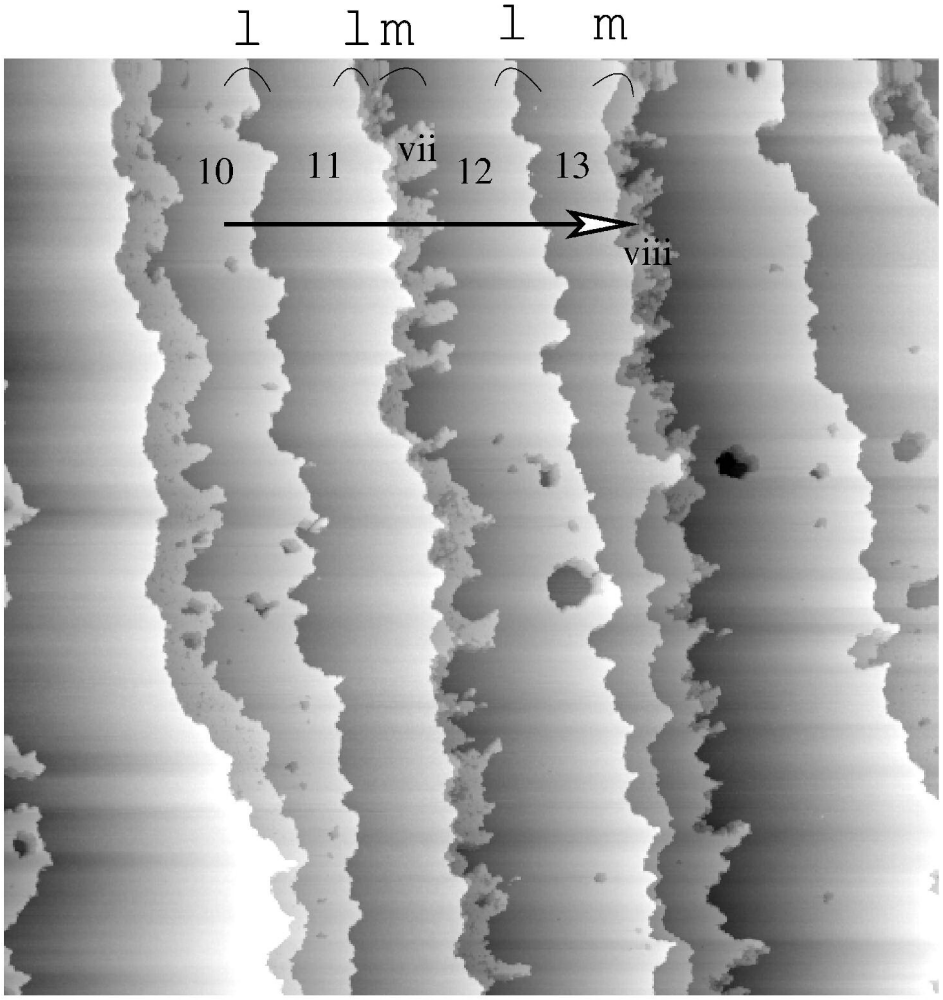

173x189mm (600 x 600 DPI)

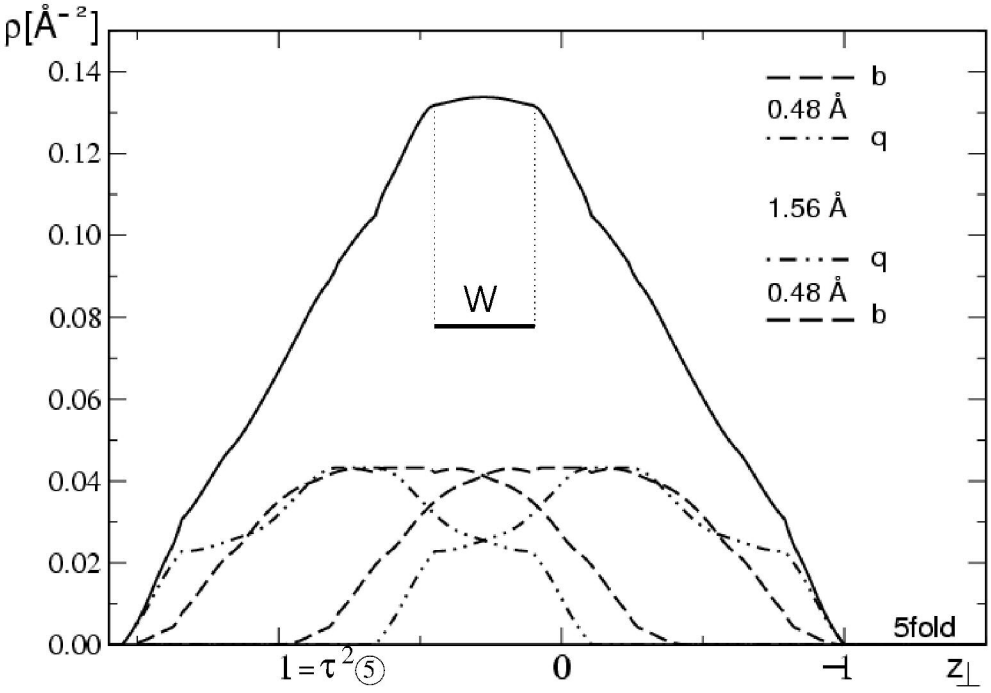

221x155mm (600 x 600 DPI)

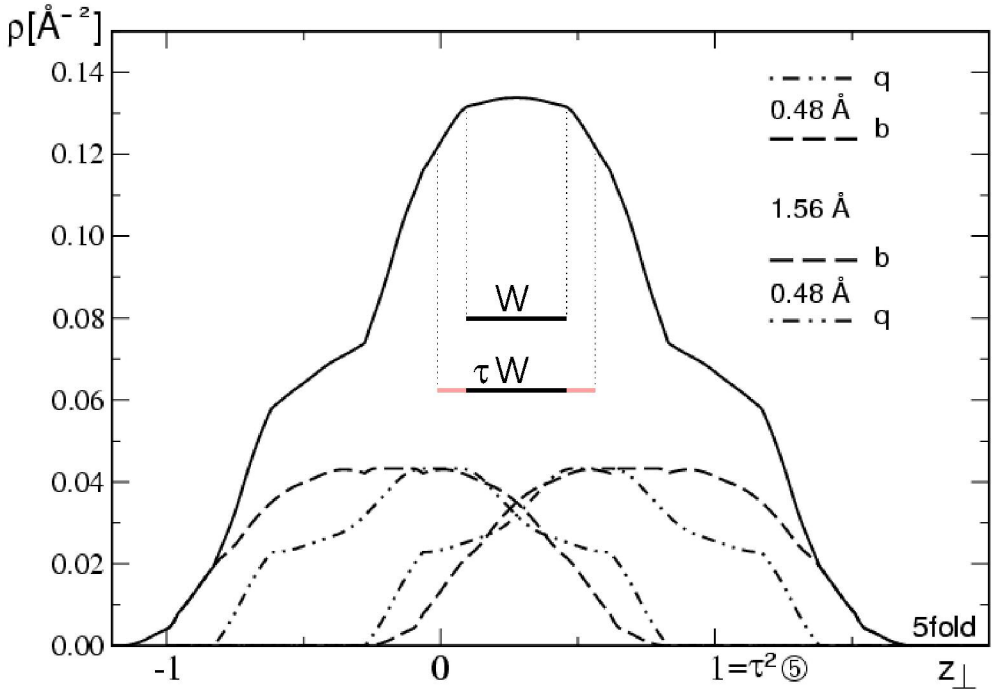

221x155mm (600 x 600 DPI)

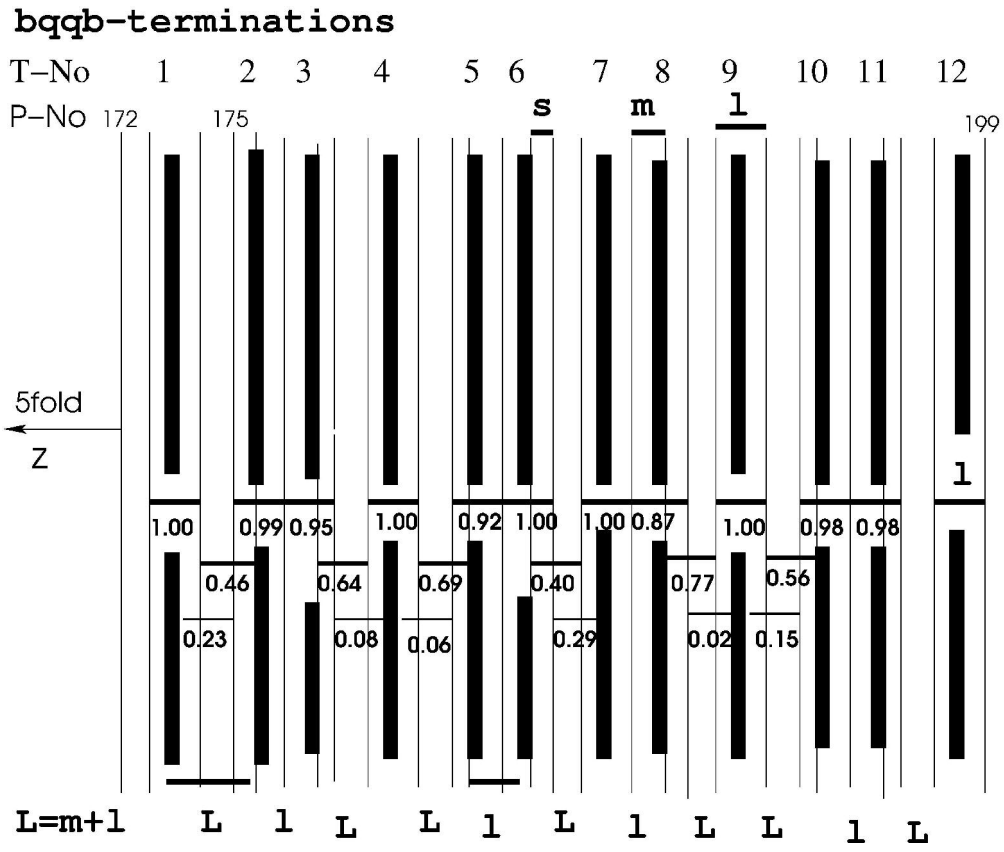

178x149mm (600 x 600 DPI)

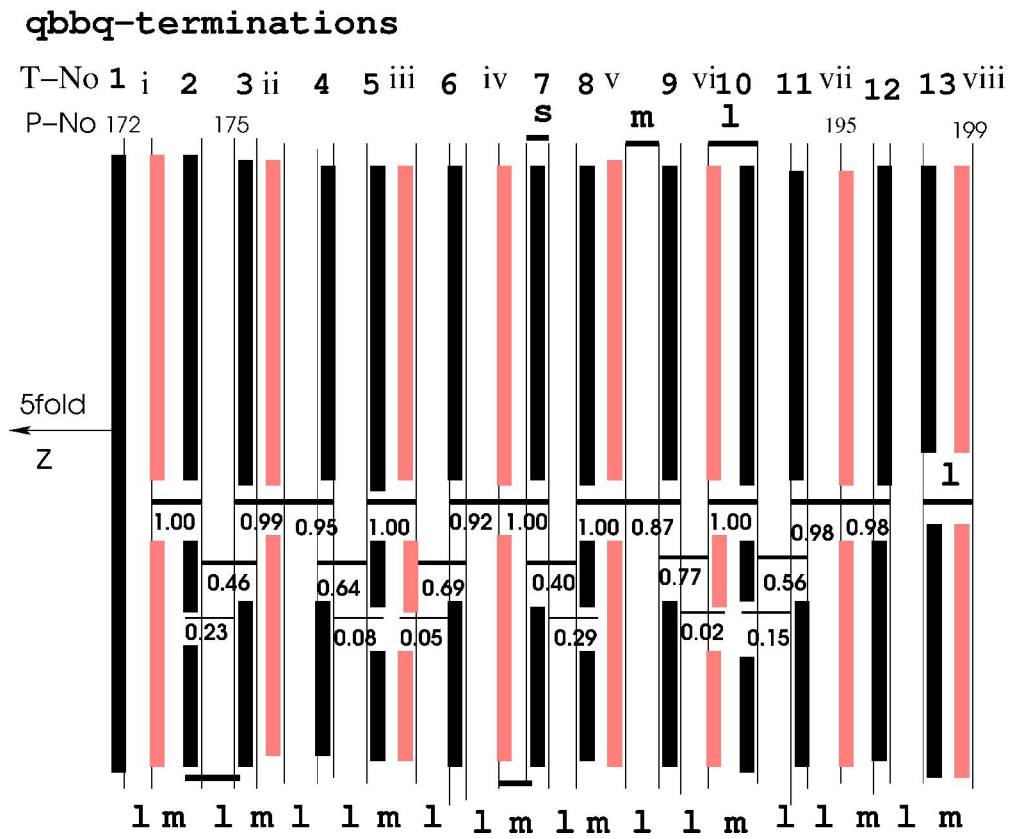

181x149mm (600 x 600 DPI)

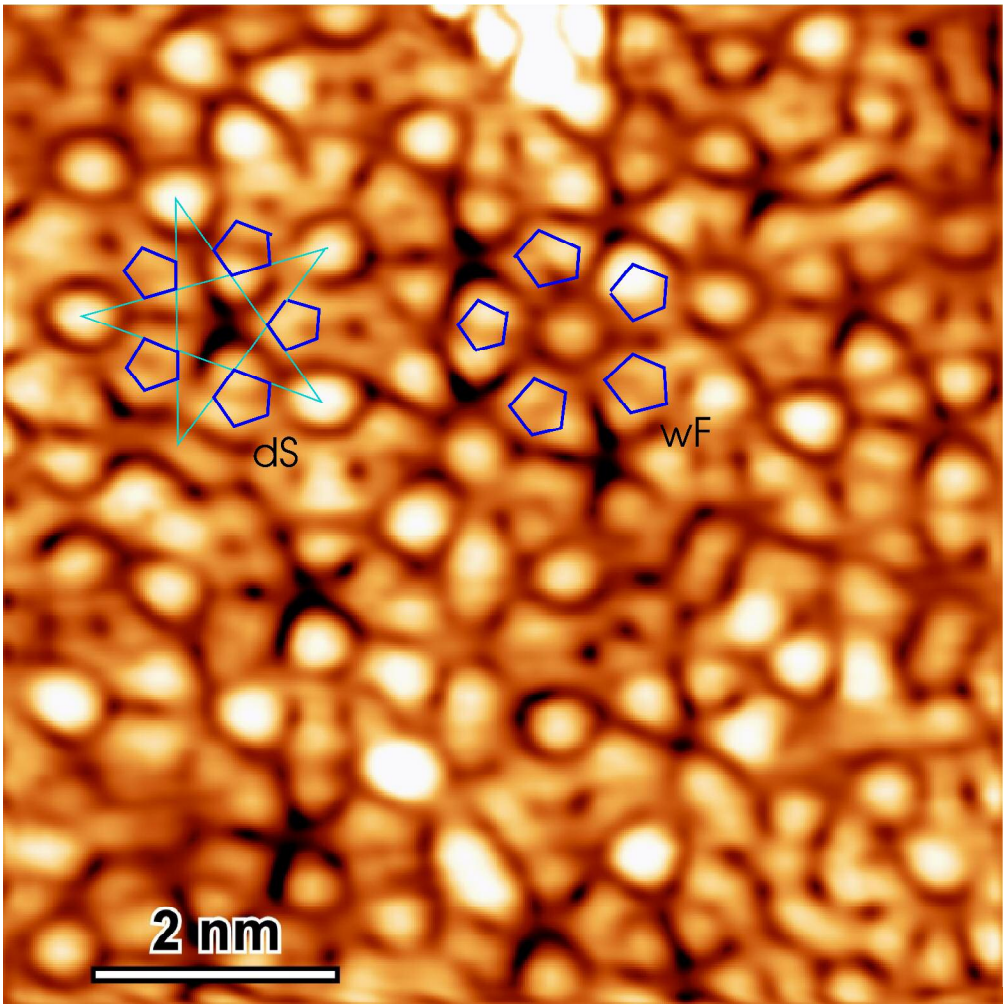

446x446mm (600 x 600 DPI)

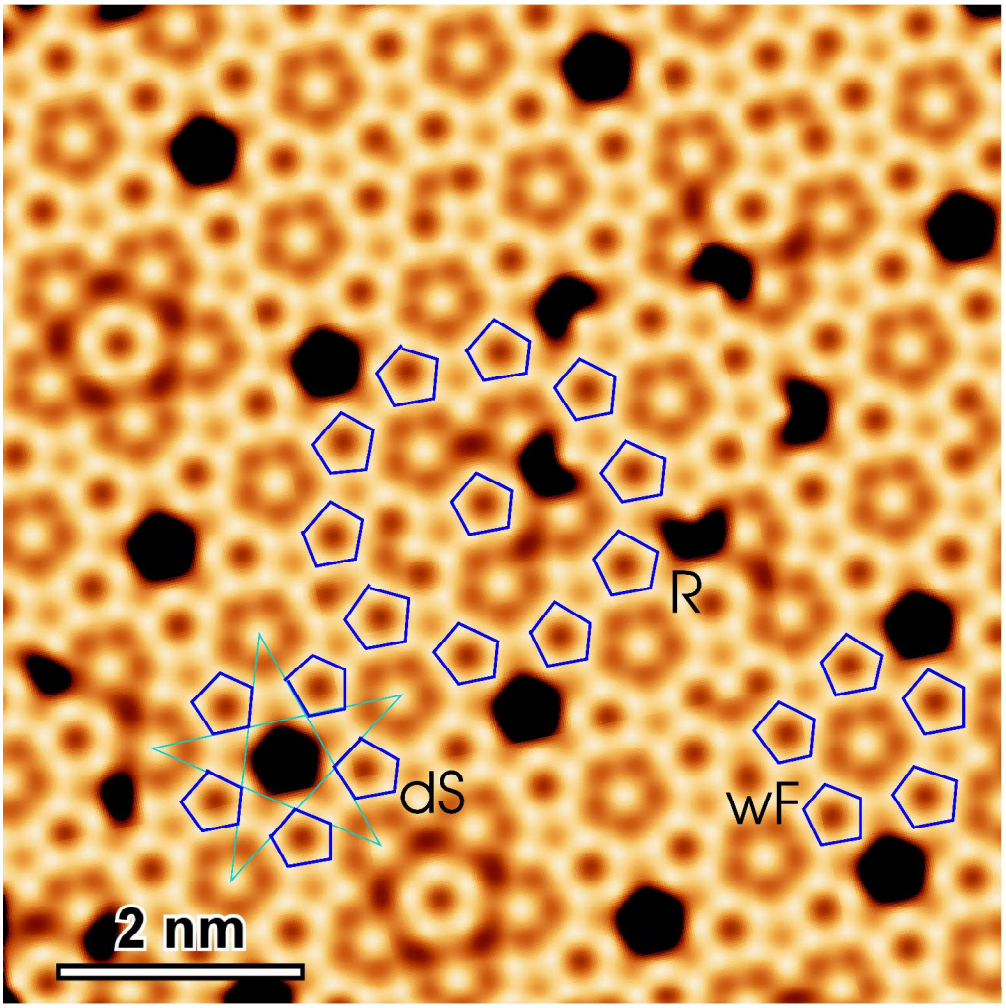

446x446mm (600 x 600 DPI)

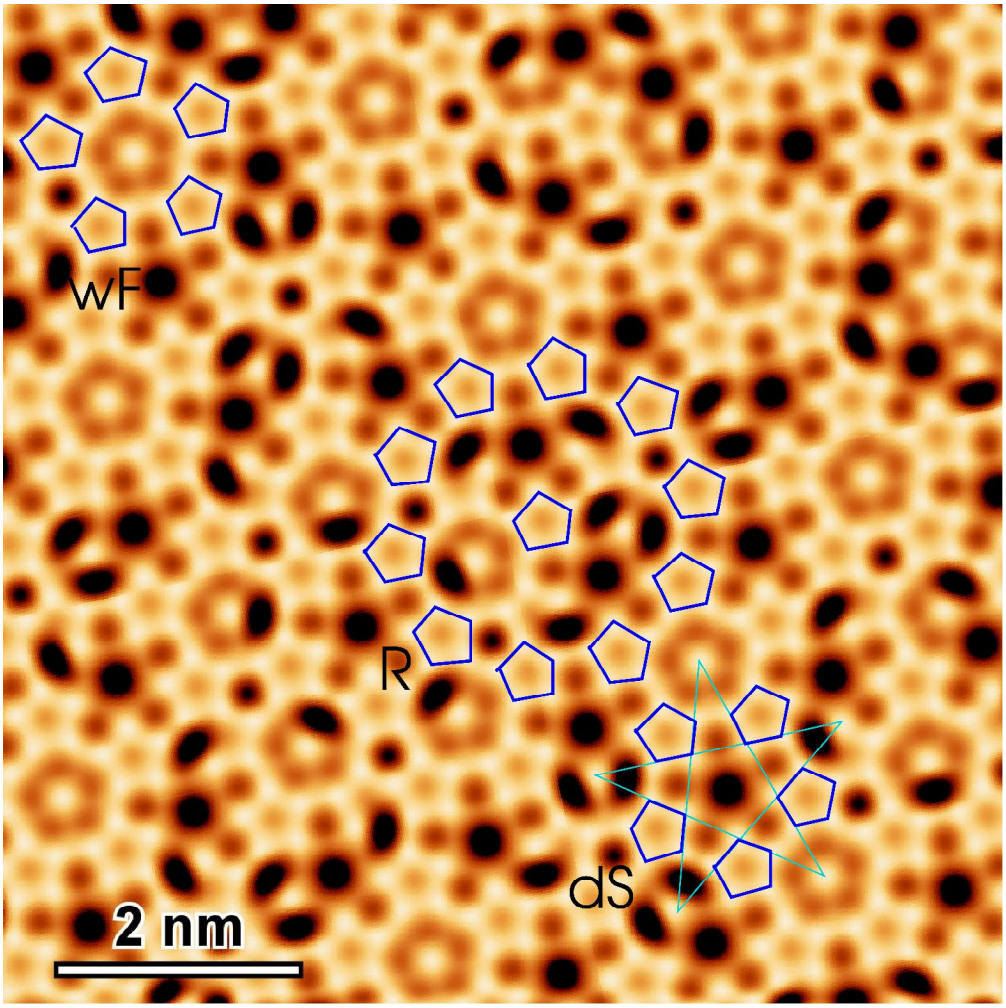

444x444mm (600 x 600 DPI)

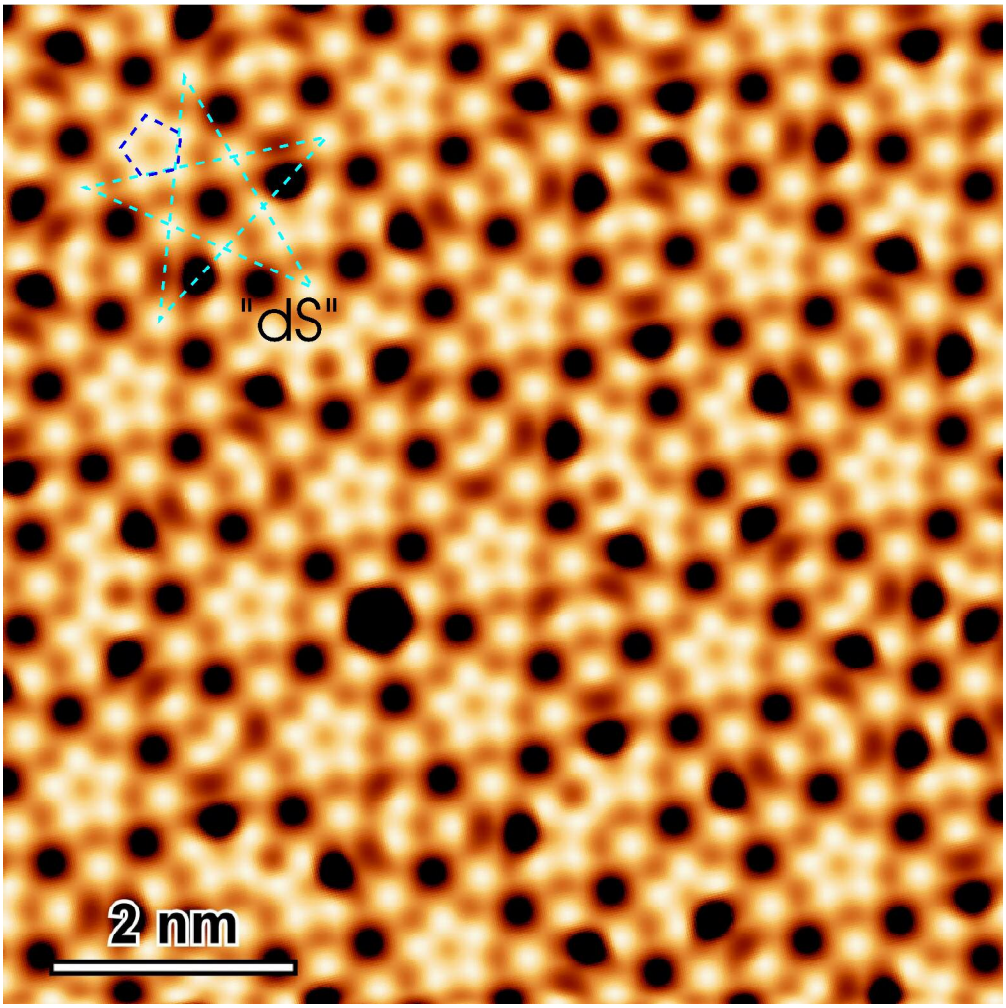

446x446mm (600 x 600 DPI)

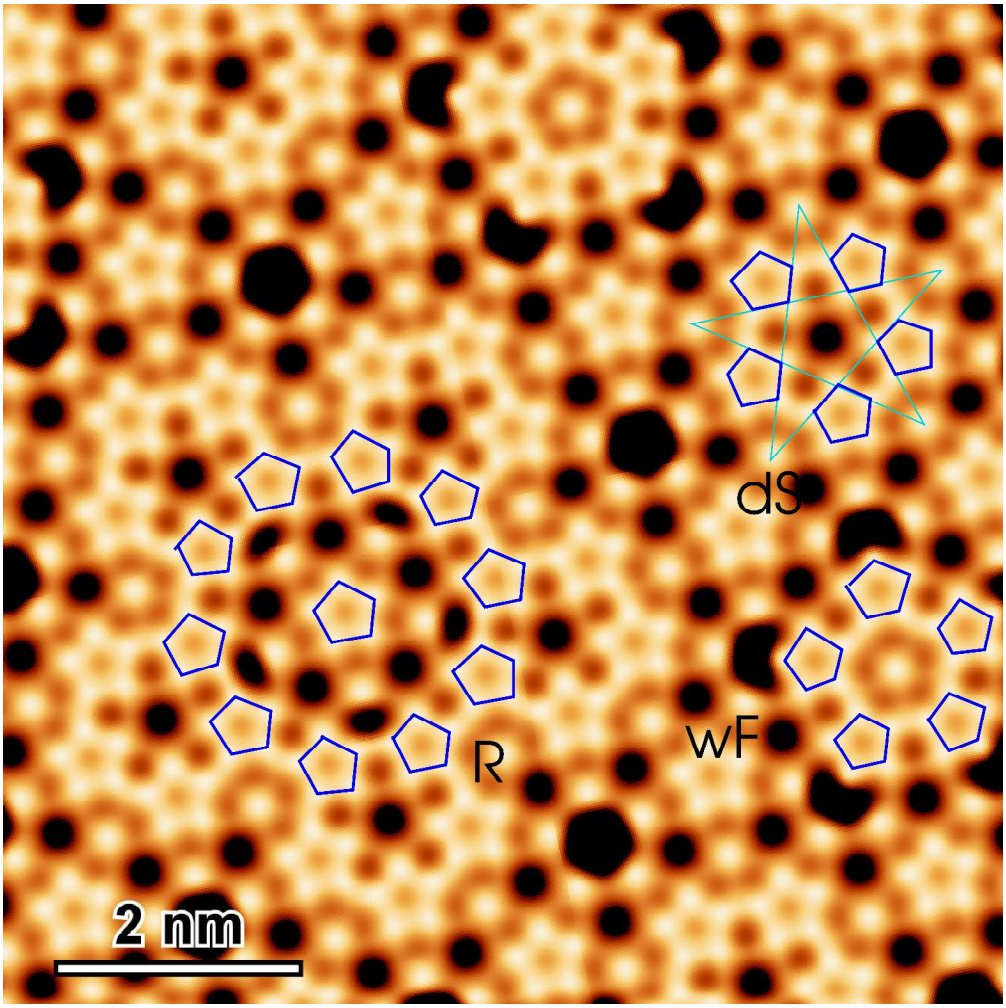

444x444mm (600 x 600 DPI)

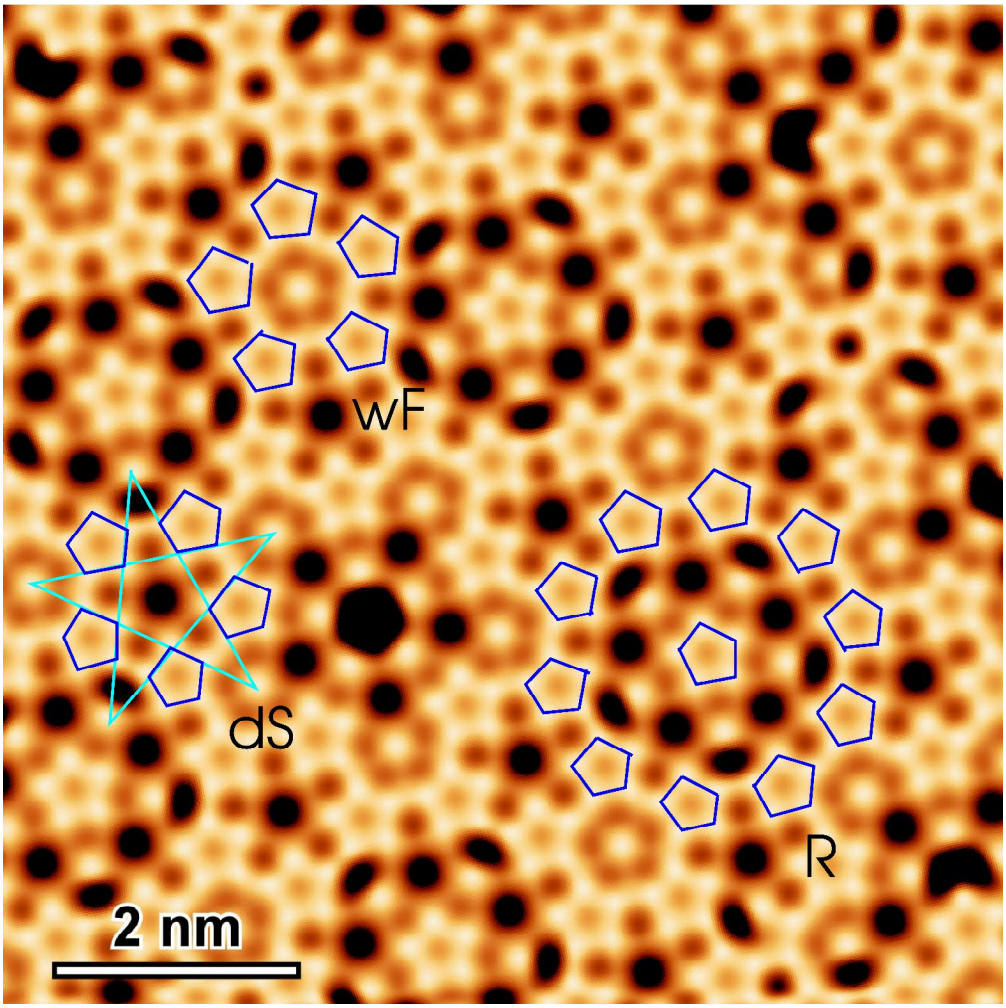

446x446mm (600 x 600 DPI)